University of Wollongong

Research Online

15-6-1998

Elementary electronic excitation in three-dimensional electron gases under free-electron laser radiations

W. Xu
University of Wollongong

Elementary electronic excitation in three-dimensional electron gases under free-electron laser radiations

W. Xu*

Department of Engineering Physics, Institute for Superconductivity and Electronic Materials, University of Wollongong, New South Wales 2522, Australia

I present a detailed theoretical study of the collective excitation associated with plasmon modes in three-dimensional electron gases (3DEG's), subject to free-electron laser (FEL) radiations. Using the exact solution of the time-dependent Schrödinger equation in which the effect of the electromagnetic (e.m.) radiation field is included in the Coulomb gauge, I have derived the Green's function, the density of states (DOS), and the density-density correlation function for free electrons in $(\mathbf{K},t)$ and $(\mathbf{K},\Omega)$ representation. With these results, the influence of the FEL radiations on plasmon spectrum in a 3DEG has been studied by employing the random-phase approximation. It has been found that the presence of the linearly polarized terahertz laser fields will lead to a strong modulation of the electron DOS and of the Fermi energy in a 3DEG structure. As a consequence, the plasmon spectrum in an electron gas can be tuned by varying the intensity and/or frequency of the e.m. radiation. A number of important and distinctive effects induced by the FEL radiations are presented and discussed. [S0163-1829(98)05424-1]

I. INTRODUCTION

The investigation of collective excitations in electron gases, such as plasmons, phonons, magnons, and nuclear quanta, has played an important role in modern condensed-matter physics and electronics. It is well known that in a high-density electron gas, the electronic transitions via spin- and charge-density oscillations will result in an elementary excitation associated with plasmon oscillation modes. Experimentally, both far-infrared-absorption spectroscopy and inelastic-resonant-light-scattering spectroscopy have been used extensively to measure and to study the elementary excitation spectra in electronic devices such as semiconductor systems.[1] In these optical measurements, the intensity of the electromagnetic (e.m.) radiation applied is relatively weak so that the probing fields do not vary the excitation spectrum and one may *assume* that the radiation field affects very weakly the basic electronic structure of the device system. In the absence of the intense e.m. radiations, plasmons in three-dimensional electron gases[2] (3DEG's) and in low-dimensional electronic systems[3–5] have been studied in detail in the past, both experimentally and theoretically, and the results are well documented in the literature.[2–5]

In recent years, there has been a rapid expansion in developing high-power and long-wavelength laser sources such as free-electron lasers (FEL's). At present, the powerful far-infrared (FIR) or terahertz (10^{12} Hz) FEL's have become available at, e.g., the University of California, Santa Barbara[6–8] and the Free Electron Laser for Infrared Experiments, the Netherlands.[9–11] The current generation of the FEL's has already been able to provide the tunable source of linearly polarized terahertz radiations. Using the sources of the FEL radiation, one can study the dependence of the physical properties in an electronic device on frequency and strength of the linearly polarized e.m. radiation. Recently, experimental measurements have been carried out in investigating the nonlinear response of the semiconductor devices to the terahertz FEL radiations. Some important and interest-

ing phenomena, such as resonant absorption of the terahertz radiation,[6] photon-enhanced hot-electron effect,[7] terahertz-photon-induced impact ionization,[8] LO-phonon bottleneck effect,[9] terahertz-photon-assisted resonant tunneling,[10] and terahertz cyclotron resonance,[11] were observed in different semiconductor systems. It can be foreseen that the study of terahertz-driven electron gases, using FEL radiations, will make a significant impact on the investigation and characterization of condensed-matter materials such as low-dimensional semiconductor systems and nanostructures.

At present, most of the research work on terahertz-driven electron gases is focused on two-dimensional electronic systems (2DES's) such as GaAs-based heterojunctions and quantum wells. To have a better understanding of the electronic and optical properties observed experimentally in dimensionally reduced systems such as 2DES's, it is important to be able to know how an ideal 3DEG responses to such intense terahertz e.m. field as provided by the FEL radiations, and this is the main motivation of the present study. When a 3DEG, realized from, e.g., a semiconductor system, is subjected to intense terahertz e.m. field, the electron kinetic energy, the Fermi energy, the plasmon energy, the phonon energy, etc., in the system can be comparable to the photon energy and to the energy of the radiation field. This implies that the terahertz e.m. field may couple strongly to the electronic system and, as a result, may vary significantly the electronic structure of the device system. This has been verified by a pioneering work done by Jauho and Johnsen.[12] In the presence of the linearly polarized e.m. radiations, the electron density of states (DOS) in ideal 3DEG and 2DEG structures has been investigated recently[12] by using the approach of the gauge-invariant spectral function. An important radiation effect, such as the blueshift of the absorption edge arisen from the dynamic Franz-Keldysh effect, has been predicted theoretically.[12] From the fact that the collective excitations, such as plasmons, depend strongly on the electronic structure and on the electronic property of the device system, one would expect that under the intense terahertz

e.m. radiations the plasmon modes generated from an electronic device may differ significantly from those observed in the absence of the radiation field.

So far, little theoretical work has been conducted regarding the collective excitations in electron gases in the presence of the intense e.m. radiations. This paper attempts to make a contribution to this topic, through examining the dependence of the plasmon spectrum on intensity and frequency of the FEL radiations. In the present study, I consider a rather simple theoretical approach to calculate the Green's function (see Sec. II), the DOS (see Sec. III), and the density-density correlation function (see Sec. IV) for noninteracting electrons in a 3DEG subjected to e.m. radiations. Using the results obtained, in Sec. V, I perform a detailed study of the influence of the terahertz e.m. radiations on the dielectric response function and the plasmon spectrum in a GaAs-based 3DEG system. The conclusions obtained from this study are summarized in Sec. VI.

II. GREEN'S FUNCTION

When an ideal 3DEG is subjected to an e.m. field polarized along the x axis, the single-electron Hamiltonian to describe the electron-photon system can be written as

$$H_0(t) = \frac{[p_x - eA(t)]^2 + p_y^2 + p_z^2}{2m^*}. \quad (1a)$$

Here a parabolic-conduction-band structure has been considered, $p_x = -i\hbar \partial/\partial x$ is the momentum operator, $\mathbf{A}(t) = (A(t),0,0)$ is the vector potential induced by the e.m. radiation field polarized along the x direction, and m^* is the effective electron mass. Furthermore, I have used the Coulomb gauge[13] to describe the e.m. field. The usage of the Coulomb gauge allows us to choose the vector potential $\mathbf{A}$ and the scalar potential ϕ for the radiation field such that $\boldsymbol{\nabla} \cdot \mathbf{A} = 0$ and $\phi = 0$. These gauge conditions correspond to a situation where the charge density $\rho = 0$ and the current density $\mathbf{j} = \mathbf{0}$, which are true for the case of free electrons in a 3DEG in the absence of scattering, inhomogeneity, external driving field, etc. After using the dipole approximation for the radiation field and taking $A(t) = A_0 \sin(\omega t)$, with ω being the frequency of the radiation, the solution of the time-dependent Schrödinger equation

$$i\hbar \frac{\partial \Psi(\mathbf{R},t)}{\partial t} = H_0(t)\Psi(\mathbf{R},t) \quad (1b)$$

is obtained as

$$\Psi_{\mathbf{K}}(\mathbf{R},t) = \Psi_{\mathbf{K}}(\mathbf{R},0)e^{-i[E(\mathbf{K}) + 2\gamma\hbar\omega]t/\hbar}$$
$$\times e^{ir_0 k_x[1 - \cos(\omega t)]} e^{i\gamma \sin(2\omega t)}, \quad (2a)$$

where

$$\Psi_{\mathbf{K}}(\mathbf{R},0) = e^{i\mathbf{K}\cdot\mathbf{R}}. \quad (2b)$$

Here $\mathbf{R} = (x,y,z)$, $\mathbf{K} = (k_x,k_y,k_z)$ is the electron wave vector, $E(\mathbf{K}) = \hbar^2 K^2/2m^*$ is the energy spectrum of the 3DEG, $r_0 = eF_0/m^*\omega^2$ with F_0 being the strength of the radiation electric field, $\gamma = (eF_0)^2/8m^*\hbar\omega^3$, and $2\gamma\hbar\omega$ is the energy of the radiation field. I have used the relation $\mathbf{F}(t) = \partial\mathbf{A}(t)/\partial t = (F_0 \cos(\omega t),0,0)$ with $F_0 = \omega A_0$.

From the time-dependent electron wave function given by Eq. (2), we can calculate the probability amplitude, which describes a process that if one adds an electron in a state $|\mathbf{K}'\rangle$ at time t' to the system then the system will be in a state $|\mathbf{K}\rangle$ at time t, through

$$\int d^3\mathbf{R} \, \Psi_{\mathbf{K}'}^*(\mathbf{R},t')\Psi_{\mathbf{K}}(\mathbf{R},t) = \delta_{\mathbf{K}',\mathbf{K}}R(\mathbf{K};t,t'), \quad (3a)$$

where

$$R(\mathbf{K};t,t') = e^{-i[E(\mathbf{K}) + 2\gamma\hbar\omega](t-t')/\hbar} e^{-ir_0 k_x[\cos(\omega t) - \cos(\omega t')]}$$
$$\times e^{i\gamma[\sin(2\omega t) - \sin(2\omega t')]}. \quad (3b)$$

Hence, by definition, the retarded propagator or Green's function in $(\mathbf{K},t)$ space for non-interacting electrons is given by

$$G^+(\mathbf{K}',\mathbf{K};t > t') = \delta_{\mathbf{K}',\mathbf{K}}G^+(\mathbf{K};t > t'), \quad (4a)$$

where

$$G^+(\mathbf{K};t > t') = -\frac{i}{\hbar} \Theta(t-t')R(\mathbf{K};t,t'). \quad (4b)$$

Equation (4) is a two-time Green's function, due to the shift caused by the radiation field. Moreover, Eq. (4b) satisfies [noting $d\Theta(t-t')/dt = \delta(t-t')$]

$$\left[i\hbar \frac{\partial}{\partial t} - \frac{[\hbar\mathbf{K} - e\mathbf{A}(t)]^2}{2m^*} \right] G^+(\mathbf{K};t > t') = \delta(t-t') \quad (5a)$$

in $(\mathbf{K},t)$ space and

$$\left[i\hbar \frac{\partial}{\partial t} - H_0(t) \right] G^+(\mathbf{K};t > t')\Psi_{\mathbf{K}}(\mathbf{R},0) = \delta(t-t')\Psi_{\mathbf{K}}(\mathbf{R},0)$$
$$(5b)$$

in real space, where $\mathbf{K}$ is the quantum number. So $G^+(\mathbf{K};t > t')$ is the actual Green's function in the $(\mathbf{K},t)$ representation. Similarly, we can also calculate the probability amplitude for a process that if one removes an electron (or adds a hole) in a state $|\mathbf{K}'\rangle$ at time t' to the system then the system will be in a state $|\mathbf{K}\rangle$ at time t. Thus the advanced propagator or Green's function for free electrons in the $(\mathbf{K},t)$ representation is obtained as

$$G^-(\mathbf{K}',\mathbf{K};t > t') = \delta_{\mathbf{K}',\mathbf{K}}G^-(\mathbf{K};t > t'), \quad (6a)$$

where

$$G^-(\mathbf{K};t > t') = \frac{i}{\hbar} \Theta(t-t')R(\mathbf{K};t',t). \quad (6b)$$

The Fourier transform (or average over time $t - t'$) of the retarded Green's function is given, after generating $e^{ix \cos y}$ and $e^{ix \sin y}$ into the Bessel functions, by

$$G_{\mathbf{K}}^{+}(E,t') = \int_{-\infty}^{\infty} d(t-t') e^{i(E+i\delta)(t-t')/\hbar} G^{+}(\mathbf{K};t>t')$$

$$= \sum_{m=-\infty}^{\infty} \frac{\mathcal{F}_m(k_x,t')}{E-E(\mathbf{K})-2\gamma\hbar\omega-m\hbar\omega+i\delta}, \quad (7)$$

where an infinitesimal quantity $i\delta$ has been introduced to make the integral converge. Here

$$\mathcal{F}_m(k_x,t') = (-1)^m F_m(k_x) \sum_{n=-\infty}^{\infty} i^n J_{m+n}(r_0 k_x)$$

$$\times e^{i[n\omega t' - \gamma \sin(2\omega t')]}, \quad (8a)$$

where $\mathrm{Re}\,\mathcal{F}_m(-k_x,t') = \mathrm{Re}\,\mathcal{F}_m(k_x,t')$, $\mathrm{Im}\,\mathcal{F}_m(-k_x,t') = -\mathrm{Im}\,\mathcal{F}_m(k_x,t')$, $J_m(x)$ is a Bessel function, and

$$F_m(k_x) = \sum_{n=0}^{\infty} \frac{J_n(\gamma)}{1+\delta_{n,0}} [J_{2n-m}(r_0 k_x)$$

$$+ (-1)^{m+n} J_{2n+m}(r_0 k_x)]. \quad (8b)$$

To study the steady-state properties, we can average the initial time t' over a period of the radiation field. The averaged Green's function then becomes

$$G_{\mathbf{K}}^{*}(E) = \frac{\omega}{2\pi} \int_{-\pi/\omega}^{\pi/\omega} dt' G_{\mathbf{K}}^{+}(E,t')$$

$$= \sum_{m=-\infty}^{\infty} \frac{F_m^2(k_x)}{E-E(\mathbf{K})-2\gamma\omega-m\hbar\omega+i\delta}. \quad (9)$$

One can find that the energy sum rule for this Green's function is exhausted by the imaginary part alone, i.e., $\int_{-\infty}^{\infty} dE \, \mathrm{Re}\, G_K^*(E) = 0$ and $\int_{-\infty}^{\infty} dE \, \mathrm{Im}\, G_K^*(E) = -\pi$, after using the identity $\sum_{m=-\infty}^{\infty} F_m^2(k_x) = 1$. Equation (9) is the steady-state Green's function in the $(\mathbf{K},\Omega)$ representation.

When a 3DEG is subjected to a linearly polarized e.m. radiation field, the electron wave function can be characterized by a Floquet state,[14] which is the analog to a Bloch state when replacing a spatially periodic potential with a time periodic one. As can be seen in Eq. (2a), the coupling of the radiation field to the electronic system results in the following: (i) The energy of the electronic system becomes $E(\mathbf{K}) + 2\gamma\hbar\omega$, shifted by a positive energy $2\gamma\hbar\omega = (eF_0)^2/4m^*\omega^2$ arisen from the e.m. radiation. This type of blueshift has been observed in, e.g., the dynamical Franz-Keldysh effect.[12] (ii) The time evaluation of the electron wave function will no longer be in the form $\Psi \sim e^{iEt/\hbar}$ due to the time shift caused by the time-dependent driving field. (iii) An anisotropic nature of the wave function can be observed. The physical reason behind this is that the linearly polarized radiation field has broken the symmetry of the sample geometry. As a result, the Green's functions given above are also anisotropic, i.e., depending on k_x.

In the presence of the e.m. radiations, electrons in the system can interact with the radiation field, accompanied by the processes of absorption and emission of photons by electrons. In the Green's functions given above, $m = 1,2,3,\ldots$ $(-1,-2,-3,\ldots)$ corresponds to the absorption (emission) of one, two, three, etc., photons with the frequency ω. This
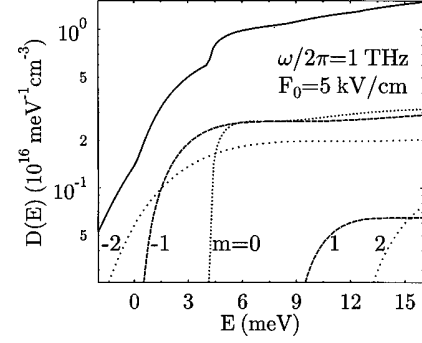

FIG. 1. Contribution from different optical processes to the electron density of states at a fixed radiation field with intensity F_0 and frequency ω. $m>0$ and $m<0$ correspond, respectively, to the channels of m-photon absorption and emission. When $F_0 = 5$ kV/cm and $\omega/2\pi = 1$ THz, $\hbar\omega \simeq 4.14$ meV and $2\gamma\hbar\omega \simeq 4.19$ meV.

also reflects the fact that the emission and absorption of photons by electrons can be achieved via multiphoton channels where $|m|>1$. When $F_0 = 0$ (and thus $r_0 = \gamma = 0$), due to the feature $J_m(0) = \delta_{m,0}$, the Green's functions given above become the well-known results obtained in the absence of the e.m. radiation.

III. DENSITY OF STATES AND FERMI ENERGY

In the study of an electron gas driven by an e.m. radiation field, the electron DOS is one of the central quantities to determine and to understand almost all physically measurable properties. In the $(\mathbf{K},\Omega)$ representation, the electron DOS is determined by the imaginary part of the Fourier transform of the Green's function, namely,

$$D(E) = -\frac{g_s}{\pi} \sum_{\mathbf{K}} \mathrm{Im}\, G_{\mathbf{K}}^*(E)$$

$$= \frac{1}{2\pi^2} \left(\frac{2m^*}{\hbar^2}\right)^{3/2} \sum_{m=-\infty}^{\infty} \Theta(E-2\gamma\hbar\omega-m\hbar\omega)$$

$$\times \sqrt{E-2\gamma\hbar\omega-m\hbar\omega}\; R_m(E-2\gamma\hbar\omega-m\hbar\omega),$$

$$(10a)$$

where $g_s = 2$ accounts for the spin degeneracy and

$$R_m(x) = \int_0^1 dy\, F_m^2\left(y\sqrt{\frac{2m^*x}{\hbar^2}}\right). \quad (10b)$$

When $F_0 = 0$, so that $r_0 = \gamma = 0$ and $R_m(x) = \delta_{m,0}$, Eq. (10) becomes the well-known result for electron DOS in the absence of the e.m. radiation, i.e.,

$$\lim_{F_0 \to 0} D(E) = \frac{1}{2\pi^2} \left(\frac{2m^*}{\hbar^2}\right)^{3/2} \Theta(E) \sqrt{E}. \quad (11)$$

The contribution due to different optical processes to the electron DOS is shown in Fig. 1 at a fixed radiation field. From Eq. (10a) we see that the contribution to the DOS from the process of m-photon absorption ($m>0$) or emission ($m<0$) becomes possible when the condition $E-2\gamma\hbar\omega -m\hbar\omega \geq 0$ is satisfied. With increasing electron energy E,
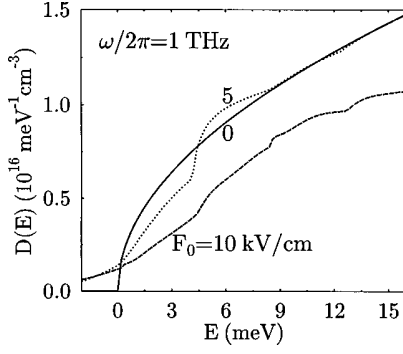
FIG. 2. Electron density of states as a function of electron energy E at a fixed radiation frequency ω for different strengths of the radiation field F_0.

FIG. 3. Density of states for electrons in GaAs as a function of electron energy E at a fixed radiation intensity F_0 for different radiation frequencies ω.

the opening up of the new channels for optical absorption and/or emission leads to an increase in the DOS. In contrast to the case of $F_0 = 0$ [see Fig. 2 and Eq. (11)], the electron DOS for a 3DEG under an e.m. radiation can be present in the energy regime $E < 0$. This arises from the processes of the photon emission, as can be seen in Fig. 1. From Fig. 1 we note that (i) in the presence of the e.m. radiations, a non-$E^{1/2}$ dependence of the DOS can be observed; (ii) in the low-energy regime, the electron DOS comes mainly from the processes of the photon emission; (iii) in the energy regime $E \sim 2\gamma\hbar\omega$, the contribution to the DOS from a process of $(|m| + 1)$-photon emission is smaller than that from an $|m|$-photon emission process; and (iv) the contribution due to the processes of multiphoton absorption can only be observed weakly in high-energy regime. Hence, in low-energy regime, which is more possibly occupied by electrons, the electron DOS comes mainly from the processes of photon emission.

The numerical results of this paper pertain to GaAs-based 3DEG structures. For GaAs, the effective electron mass is $m^* = 0.0665m_e$, with m_e being the rest electron mass, and the dielectric constant is $\kappa = 12.9$. In all of the calculations in this paper I consider n-type-doped GaAs with the typical electron density $n_e = 10^{17}$ cm^{-3}. To calculate $F_m(x)$ given by Eq. (8b), I have taken $n = 0,1,2,\ldots,20$. Furthermore, the contributions from $m = 0, \pm 1, \pm 2, \ldots, \pm 20$ are included in the calculations. The inclusion of more m and n affects only the results in low-frequency radiations.

The influence of the strength and frequency of the terahertz radiation field on the electron DOS in 3DEG structure is shown in Figs. 2 and 3. With increasing radiation intensity F_0 and/or decreasing radiation frequency ω, the DOS in high-energy regime decreases, mainly due to the increase in γ and r_0. For the case of very low-frequency radiations (e.g., $\omega/2\pi = 0.5$ THz in Fig. 3), the contributions from multiphoton emission and absorption to the DOS can become larger in comparison to the situation of high-frequency radiations. Under the relatively low-frequency radiations, the electrons can interact with the radiation field via multiphoton channels because of relatively small energy transfer. The theoretical results obtained in this paper agree with those observed in the dynamical Franz-Keldysh effect in a 3DEG system.[12]

The results shown above indicate that the processes of optical absorption and emission may result in an increase in the DOS. However, due to the blueshift by the energy $2\gamma\hbar\omega$
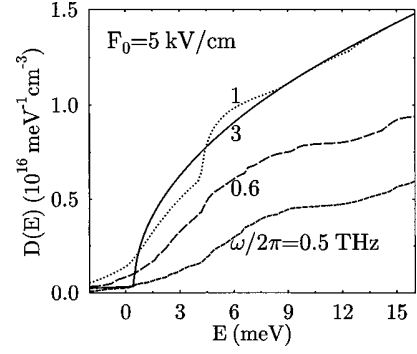
of the radiation field and to the feature $|J_m(x)| \leqslant 1$, the overall DOS for electrons in a relatively high-energy regime will be reduced in comparison to that at $F_0 = 0$ (see Fig. 2). This effect is more pronounced for high-intensity and low-frequency radiations. The electron DOS measures the maximum number of electrons that can occupy an energy range. The e.m. field applied will drive electrons out of a certain energy regime by a factor of $2\gamma\hbar\omega$, so a reduced electron DOS in some energy regimes can be achieved. Due to the limiting feature $\lim_{x \to 0} J_m(x) = \delta_{m,0}$, for a radiation with relatively high frequency (e.g., $\omega/2\pi = 3$ THz in Fig. 3) and/or low intensity (e.g., $F_0 = 0$ in Fig. 2), which leads $r_0 \to 0$ and $\gamma \to 0$, the effects of the e.m. radiation on electron DOS can be suppressed. Moreover, because $r_0 \sim F_0/\omega^2$ and $\gamma \sim F_0^2/\omega^3$, the radiation frequency has a stronger effect on the DOS, as can be seen in Fig. 3.

A direct and important application of the electron DOS is to determine the Fermi energy of an electronic system. Using the condition of electron number conservation and assuming that the total electron density n_e in the 3DEG system is not varied by the presence of the radiation field, the Fermi energy E_F for a 3DEG subjected to an e.m. radiation can be determined by

$$n_e = \int_0^\infty dE\, f(E)D(E), \qquad (12)$$

where $f(E) = [e^{(E-E_F)/k_B T} + 1]^{-1}$ is the Fermi-Dirac function. In the low-temperature limit (i.e., $T \to 0$), we have $f(E) \to \Theta(E_F - E)$ and

$$n_e = \frac{1}{3\pi^2}\left(\frac{2m^*}{\hbar^2}\right)^{3/2} \sum_m \Theta(E_F - 2\gamma\hbar\omega - m\hbar\omega)$$
$$\times (E_F - 2\gamma\hbar\omega - m\hbar\omega)^{3/2} S_m(E_F - 2\gamma\hbar\omega - m\hbar\omega),$$
$$(13a)$$

where

$$S_m(x) = \frac{3}{2}\int_0^1 dy(1-y^2)F_m^2\left(y\sqrt{\frac{2m^*x}{\hbar^2}}\right). \qquad (13b)$$

When $F_0 = 0$, we have $S_m(x) = \delta_{m,0}$ and $n_e = K_F^3/3\pi^2$, where $K_F = (2m^*E_F/\hbar^2)^{1/2}$.
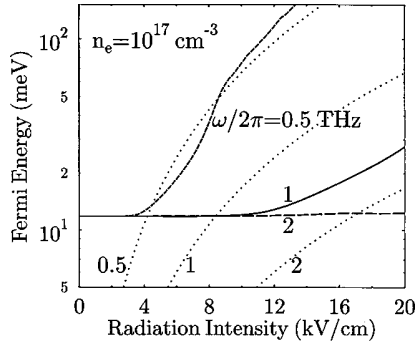
FIG. 4. Fermi energy as a function of radiation intensity F_0 for different radiation frequencies. n_e is the electron density of the 3DEG and dotted curves are the energies $2\gamma\hbar\omega$ of the radiation fields.

The dependence of the Fermi energy in a 3DEG on the strength and frequency of the terahertz laser fields is shown in Figs. 4 and 5, respectively. Because of the reduction of the electron DOS by the radiation field, especially at the low-frequency and high-intensity radiations, the Fermi energy increases rapidly with increasing radiation intensity and/or decreasing radiation frequency. From Eq. (13) we can find that for a radiation field with very high intensity and low frequency so that $2\gamma\hbar\omega\gg\hbar\omega$, the Fermi energy is $E_F\sim2\gamma\hbar\omega\sim(F_0/\omega)^2$, which can be seen in Figs. 4 and 5. Under the high-frequency (e.g., $\omega/2\pi>2$ THz in Fig. 5) and/or low-intensity (e.g., $F_0<2$ kV/cm in Fig. 4) e.m. radiations, the Fermi energy in a 3DEG depends very weakly on the radiation. In Figs. 4 and 5, I also plot the results for the energy $\mathcal{E}=2\gamma\hbar\omega$ of the radiation field (dotted curves). One can find that in some radiation intensity and frequency regimes, the Fermi level E_F may be below the energy of the radiation field $\mathcal{E}$. This implies that in these regimes, the processes of the photon emission will be the major channels to determine the Fermi energy. A significant conclusion that I draw from these results is that by varying the strength and frequency of the terahertz e.m. radiation, one can control the Fermi level in the device system.

The theoretical results obtained here indicate the following. (i) In high-intensity and low-frequency radiations where $\mathcal{E}\gg\hbar\omega$, the Fermi energy is determined mainly by the energy of the radiation field via the dynamical Franz-Keldysh effect. In this case, noting that $\Sigma_{m=-\infty}^{\infty}F_m^2(x)=1$, we have $n_e\simeq K_F^{*3}/3\pi^2$, where $K_F^*=[2m^*(E_F-2\gamma\hbar\omega)/\hbar^2]^{1/2}$. (ii) In the intermediate radiation intensity and frequency regime, the Fermi energy is mainly determined by the emission of the photons, including the multiphoton emission channels, which results in $E_F<\mathcal{E}$. In this case, photon absorption, which requires a relatively large energy (see Fig. 1), affects weakly the DOS and consequently affects very weakly the Fermi energy. (iii) In low-intensity and high-frequency radiations, the relatively large photon energy and small energy of the radiation field will lead to a weak interaction between electrons and photons. In this case, it is less possible for electrons to gain the energy from the radiation field, and the processes of photon emission and absorption require a large energy transfer. Therefore, a high-frequency and low-intensity e.m. field affects weakly the DOS and the Fermi energy.

IV. ELECTRON DENSITY-DENSITY CORRELATION FUNCTION

In the study of the elementary excitations and the many-body properties in an electron gas, the electron density-density (d-d) correlation function (or so-called pair bubble) plays an important role. We now derive this function for a 3DEG subjected to a linearly polarized e.m. radiation field. Here I consider a Fermi system at finite temperatures. In this case and in the absence of the electron-electron interactions, the pair bubble in the $(\mathbf{K},t)$ representation is defined as[15]

$$-i\Pi(\mathbf{Q};t,t')=-ig_s\sum_{\mathbf{K}}\frac{1}{\beta}$$

$$\times\sum_{n=-\infty}^{\infty}[iG^-(\mathbf{K};t>t')e^{-i\omega_n(t-t')}]$$

$$\times[iG^+(\mathbf{K}+\mathbf{Q};t>t')e^{i\omega_n(t-t')}], \quad (14)$$

where $\beta=1/k_BT$, $\omega_n=(2n+1)\pi/\beta$, and $\mathbf{Q}=(q_x,q_y,q_z)$. After introducing the retarded [Eq. (4b)] and advanced [Eq. (6b)] Green's functions for the case where an e.m. radiation field is present, using the usual way of introducing the modified free propagator, and employing the integral representation of the step function through

$$\Theta(t-t')=-\int_{-\infty}^{\infty}\frac{d\Omega}{2\pi i}\frac{e^{-i\Omega(t-t')}}{\Omega+i\delta}, \quad (15)$$

Eq. (14) is then in the form

$$-i\Pi(\mathbf{Q};t,t')=e^{-ir_0q_x[\cos(\omega t)-\cos(\omega t')]}$$

$$\times\int_{-\infty}^{\infty}\frac{d\Omega}{2\pi i}\Pi_0(Q,\Omega)e^{-i\Omega(t-t')}, \quad (16a)$$

where

$$\Pi_0(Q,\Omega)=-\frac{g_s}{\beta}\sum_{\mathbf{K},n}\int_{-\infty}^{\infty}\frac{d\Omega_1}{2\pi}$$

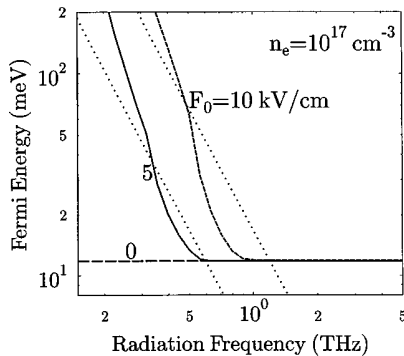$$\times\frac{1}{\hbar(\omega_n+\Omega_1)-E(\mathbf{K})-2\gamma\hbar\omega-i\delta}$$

FIG. 5. Fermi energy as a function of radiation frequency $\omega/2\pi$ for different radiation intensities. Dotted curves are the energies of the radiation fields.

$$\times \frac{1}{\hbar(\omega_n + \Omega_1 + \Omega) - E(\mathbf{K+Q}) - 2\gamma\hbar\omega + i\delta}.$$
(16b)

The method to calculate $\Pi_0(Q,\Omega)$ for a Fermi system at finite temperatures is standard and has been well documented.[15,16] Following Ref. 16, we obtain

$$\Pi_0(Q,\Omega)$$
$$= g_s \sum_{\mathbf{K}} \frac{f(E(\mathbf{K}) + 2\gamma\hbar\omega) - f(E(\mathbf{K+Q}) + 2\gamma\hbar\omega)}{\hbar\Omega + E(\mathbf{K}) - E(\mathbf{K+Q}) + i\delta},$$
(16c)

where $f(x)$ is the Fermi-Dirac function. After using Eq. (15) again, the electron d-d correlation function in the $(\mathbf{K},t)$ representation is obtained as

$$\Pi(\mathbf{Q};t,t') = g_s \frac{i}{\hbar} \Theta(t-t') e^{-ir_0 q_x[\cos(\omega t) - \cos(\omega t')]}$$

$$\times \sum_{\mathbf{K}} [f(E(\mathbf{K}) + 2\gamma\hbar\omega)$$

$$- f(E(\mathbf{K+Q}) + 2\gamma\hbar\omega)]$$

$$\times e^{-i[E(\mathbf{K+Q}) - E(\mathbf{K})](t-t')/\hbar}.$$
(17)

The Fourier transform (or average over time $t - t'$) of the electron d-d correlation function is given by

$$\Pi(\mathbf{Q};\Omega,t') = \int_{-\infty}^{\infty} d(t-t') \Pi(\mathbf{Q};t,t') e^{i(\Omega+i\delta)(t-t')}$$

$$= \sum_{m,m'=-\infty}^{\infty} i^{m'-m} J_m(r_0 q_x) J_{m'}(r_0 q_x)$$

$$\times e^{i(m+m')\omega t'} \Pi_0(Q,\Omega + m\omega).$$
(18)

At a steady state, after averaging the initial time t' over a period of the radiation field, the Fourier transform of the electron d-d correlation in the $(\mathbf{K},\Omega)$ representation is obtained as

$$\Pi(\mathbf{Q},\Omega) = \sum_{m=-\infty}^{\infty} J_m^2(r_0 q_x) \Pi_0(Q,\Omega + m\omega).$$
(19)

Here again an index m corresponds to different optical processes for emission and absorption of photons with a frequency ω, the presence of the linearly polarized radiation field results in an anisotropic d-d correlation function, and when $F_0 = 0$ so that $r_0 = \gamma = 0$ and $J_m^2(0) = \delta_{m,0}$, $\Pi(\mathbf{Q},\Omega) = \Pi_0(Q,\Omega)$ is the well-known result obtained in the absence of the e.m. radiation.

It should be noted that in the presence of the time-dependent driving field such as e.m. radiations, the electron d-d correlation function in the $(\mathbf{K},\Omega)$ representation, obtained from first handling the pair bubble in $(\mathbf{K},t)$ space and then doing the Fourier transform of it (method I), differs sharply from that obtained from first doing the Fourier transform of the Green's functions and then handling the pair bubble in the $(\mathbf{K},\Omega)$ representation (method II). In contrast,

in the absence of the radiation field, two theoretical approaches lead to an identical final result. Because we are dealing with the time-dependent problem, method I is the only way to calculate correctly the electron d-d correlation function in the $(\mathbf{K},\Omega)$ representation.

In the presence of the e.m. radiation field, the real and imaginary parts of the Fourier transform of the electron d-d correlation function are given, respectively, by

$$\Pi_1(\mathbf{Q},\Omega) = \frac{(2m^*/\hbar^2)^{3/2}}{8\pi^2 \varepsilon_Q^{1/2}} \sum_m J_m^2(r_0 q_x)$$

$$\times \int_0^{\infty} dx\, f(x + 2\gamma\hbar\omega)$$

$$\times \ln \frac{a_m^2 - \varepsilon_Q^2 - 4x\varepsilon_Q + 4\varepsilon_Q\sqrt{x\varepsilon_Q}}{a_m^2 - \varepsilon_Q^2 - 4x\varepsilon_Q - 4\varepsilon_Q\sqrt{x\varepsilon_Q}}$$
(20a)

and

$$\Pi_2(\mathbf{Q},\Omega) = -\frac{(2m^*/\hbar^2)^{3/2}}{8\pi\varepsilon_Q^{1/2}} \sum_m J_m^2(r_0 q_x)$$

$$\times \int_{(a_m - \varepsilon_Q)^2/4\varepsilon_Q}^{\infty} dx [f(x + 2\gamma\hbar\omega)$$

$$- f(x + 2\gamma\hbar\omega + a_m)].$$
(20b)

Here $\varepsilon_Q = \hbar^2 Q^2/2m^*$ and $a_m = \hbar\Omega + m\hbar\omega$. In the low-temperature limit (i.e., $T \to 0$), we have

$$\Pi_1(\mathbf{Q},\Omega) = -\frac{m^* K_F^*}{\pi^2\hbar^2} \Theta(E_F - 2\gamma\hbar\omega)$$

$$\times \sum_{m=-\infty}^{\infty} J_m^2(r_0 q_x) I_m(Q,\Omega)$$
(21a)

and

$$\Pi_2(\mathbf{Q},\Omega) = -\frac{m^*}{16\pi\hbar^2 Q^3} \Theta(E_F - 2\gamma\hbar\omega)$$

$$\times \sum_{m=-\infty}^{\infty} J_m^2(r_0 q_x) II_m(Q,\Omega).$$
(21b)

Here $K_F^* = [2m^*(E_F - 2\gamma\hbar\omega)/\hbar^2]^{1/2}$ is the radius of the effective Fermi sphere shifted by the energy of the radiation field, $q_m^2 = 2m^*(\Omega + m\omega)/\hbar$,

$$I_m(Q,\Omega) = \frac{1}{2} + \frac{4Q^2 K_F^{*2} - (Q^2 + q_m^2)^2}{16Q^3 K_F^*}$$

$$\times \ln \left| \frac{2QK_F^* + Q^2 + q_m^2}{2QK_F^* - Q^2 - q_m^2} \right| + \frac{4Q^2 K_F^{*2} - (Q^2 - q_m^2)^2}{16Q^3 K_F^*}$$

$$\times \ln \left| \frac{2QK_F^* + Q^2 - q_m^2}{2QK_F^* - Q^2 + q_m^2} \right|,$$
(21c)

and
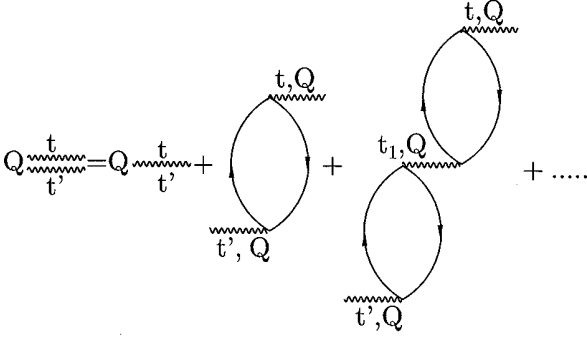
$$II_m(Q,\Omega) = \Theta[4Q^2 K_F^{*2} - (Q^2 + q_m^2)^2]$$

FIG. 6. Diagrams for the effective electron-electron interaction under the random-phase approximation in $(\mathbf{K},t)$ representation.

$$\times[4Q^2 K_F^{*2}-(Q^2+q_m^2)^2]$$
$$-\Theta[4Q^2 K_F^{*2}-(Q^2-q_m^2)^2]$$
$$\times[4Q^2 K_F^{*2}-(Q^2-q_m^2)^2]. \tag{21d}$$

Moreover, for the small Q case where $Q\ll1$, so that $|r_0 q_x|\ll1$ and $|a_m|\gg|E(\mathbf{K})-E(\mathbf{K}+\mathbf{Q})|$, the real part of the electron d-d correlation function in the $T\to0$ limit is given, after expanding it with respect to $\mathbf{Q}$, by

$$\Pi_1(\mathbf{Q},\Omega)\simeq\frac{2Q^2 K_F^{*3}}{3\pi^2(\hbar\Omega)^2}\,\Theta(E_F-2\gamma\hbar\omega)$$
$$\times\left[1+\frac{\mathcal{A}}{\Omega^2}+\mathcal{B}\,\frac{3\Omega^2-\omega^2}{(\Omega^2-\omega^2)^2}+O(\mathbf{Q}^4)\right]. \tag{22}$$

Here $\mathcal{A}=3Q^2 V_F^{*2}/5\sim Q^2$, with $V_F^*=\hbar K_F^*/m^*$ being the effective Fermi velocity, and $\mathcal{B}=(r_0 q_x)^2\omega^2/2\sim Q^2$. In Eq. (22) the term associated with $\mathcal{B}$ arises from the processes of photon emission and absorption. When the expansion is terminated with the $\mathbf{Q}^2$ terms, the optical processes associated with $m=0$ and ±1 contribute to the electron d-d correlation function. When the higher orders of $\mathbf{Q}$ are taken into account, more optical channels have to be included.

V. PLASMON SPECTRUM

A. Dynamical dielectric function

With the electron d-d correlation function given above, we can derive the dynamical dielectric function of a 3DEG in the presence of the intense e.m. radiations. In the present study, we limit ourselves to the case where the calculations are carried out within the random-phase approximation (RPA). It has been proved in the past[2-4] that the RPA dielectric function is quite accurate in the study of the plasmon spectrum in different electron gases in the absence of the intense e.m. radiation. Since we are dealing with a time-dependent problem, we have to first look into the effective electron-electron (e-e) interaction in $(\mathbf{K},t)$ space. In the $(\mathbf{K},t)$ representation, the RPA diagrams for the e-e interaction are given in Fig. 6. Using these diagrams, the effective e-e interaction can be calculated through

$$-iV_{\text{eff}}(\mathbf{Q};t,t')=[-iV(Q)]\delta(t-t')$$
$$+[-iV(Q)][-i\Pi(\mathbf{Q};t,t')][-iV(Q)]$$
$$+\int_{t'}^{t}dt_1[-iV(Q)][-i\Pi(\mathbf{Q};t_1,t')]$$
$$\times[-iV(Q)][-i\Pi(\mathbf{Q};t,t_1)][-iV(Q)]$$
$$+\cdots. \tag{23a}$$

Here $V(\mathbf{Q})$ is the space Fourier transform of the matrix element for the bare e-e interaction induced by the Coulomb potential in the second quantization representation, namely,

$$V(\mathbf{Q})=\frac{4\pi e^2}{\kappa Q^2}\int d^3\mathbf{R}_1 d^3\mathbf{R}_2|\Psi_{\mathbf{K}+\mathbf{Q}}^*(\mathbf{R}_1,t)\Psi_{\mathbf{K}}(\mathbf{R}_1,t)|$$
$$\times|\Psi_{\mathbf{K}}^*(\mathbf{R}_2,t)\Psi_{\mathbf{K}+\mathbf{Q}}(\mathbf{R}_2,t)|e^{i\mathbf{Q}\cdot(\mathbf{R}_1-\mathbf{R}_2)}$$
$$=\frac{4\pi e^2}{\kappa Q^2}, \tag{23b}$$

where κ is the dielectric constant. In $(\mathbf{K},t)$ space, $V(\mathbf{Q})$ is independent of t, which is in line with the fact that the bare e-e interaction in an electronic system is time independent. Introducing the pair bubble obtained in $(\mathbf{K},t)$ space [see Eq. (17)] into Eq. (23a), the effective e-e interaction can be written as

$$V_{\text{eff}}(\mathbf{Q};t,t')=\frac{V(Q)}{\epsilon(\mathbf{Q};t,t')}. \tag{24}$$

Hence, by definition, the inverse dielectric function of an electron gas in $(\mathbf{K},t)$ space is obtained as

$$\frac{1}{\epsilon(\mathbf{Q};t,t')}=\delta(t-t')+\frac{i}{\hbar}\,\Theta(t-t')$$
$$\times e^{-ir_0 q_x[\cos(\omega t)-\cos(\omega t')]}$$
$$\times\sum_{j=1}^{\infty}[-g_s V(Q)]^j I_j(\mathbf{Q};t,t'). \tag{25}$$

Using the notations

$$\Delta f_j=f(E(\mathbf{K}_j)+2\gamma\hbar\omega)-f(E(\mathbf{K}_j+\mathbf{Q})+2\gamma\hbar\omega) \tag{26a}$$

and

$$\Delta E_j=E(\mathbf{K}_j+\mathbf{Q})-E(\mathbf{K}_j), \tag{26b}$$

the functional form of $I_j(\mathbf{Q};t,t')$ in Eq. (25) is given by

$$I_1(\mathbf{Q};t,t')=\sum_{\mathbf{K}_1}\Delta f_1 e^{-i\Delta E_1(t-t')/\hbar}, \tag{27a}$$

$$I_2(\mathbf{Q};t,t')=\sum_{\mathbf{K}_1,\mathbf{K}_2}\Delta f_1\Delta f_2\left[\frac{e^{-i\Delta E_1(t-t')/\hbar}}{\Delta E_1-\Delta E_2}+\frac{e^{-i\Delta E_2(t-t')/\hbar}}{\Delta E_2-\Delta E_1}\right], \tag{27b}$$

and

$$I_j(\mathbf{Q};t,t') = \sum_{\mathbf{K}_1,\mathbf{K}_2,\ldots,\mathbf{K}_j} \Delta f_1 \Delta f_2 \cdots \Delta f_j$$
$$\times \left[\frac{e^{-i\Delta E_1(t-t')/\hbar}}{(\Delta E_1 - \Delta E_2) \cdots (\Delta E_1 - \Delta E_j)} \right.$$
$$\left. + \cdots + \frac{e^{-i\Delta E_j(t-t')/\hbar}}{(\Delta E_j - \Delta E_{j-1}) \cdots (\Delta E_j - \Delta E_1)} \right].$$
$$\tag{27c}$$

The Fourier transform of the inverse dielectric function is given, after generating $e^{ix\cos y}$ in Eq. (25) into the Bessel functions, by

$$\frac{1}{\epsilon(\mathbf{Q},\Omega;t')} = \int_{-\infty}^{\infty} d(t-t') \frac{1}{\epsilon(\mathbf{Q};t,t')} e^{i(\Omega+i\delta)(t-t')}$$
$$= \sum_{m,m'=-\infty}^{\infty} \frac{i^{m'-m} J_m(r_0 q_x) J_{m'}(r_0 q_x) e^{i(m+m')\omega t'}}{1 - V(Q)\Pi_0(Q,\Omega+m\omega)},$$
$$\tag{28}$$

where $\Pi_0(Q,\Omega)$ is given by Eq. (16c). At a steady state, after averaging the initial time t' over a period of the radiation field, the Fourier transform of the inverse dielectric function of a 3DEG under an e.m. radiation is obtained, in the $(\mathbf{K},\Omega)$ representation, as

$$\frac{1}{\epsilon(\mathbf{Q},\Omega)} = \frac{\omega}{2\pi} \int_{-\pi/\omega}^{\pi/\omega} \frac{dt'}{\epsilon(\mathbf{Q},\Omega;t')}$$
$$= \sum_{m=-\infty}^{\infty} \frac{J_m^2(r_0 q_x)}{1 - V(Q)\Pi_0(\mathbf{Q},\Omega+m\omega)}. \tag{29}$$

Here, once more, the index m corresponds to the process of the emission ($m<0$) or absorption ($m>0$) of m photons, the presence of the radiation field results in an anisotropic dielectric function that depends on q_x, and when $F_0=0$, so $r_0=\gamma=0$ and $J_m^2(0)=\delta_{m,0}$, $\epsilon(\mathbf{Q},\Omega)=1-V(Q)\Pi_0(Q,\Omega)$ is the well-known result obtained in the absence of the e.m. radiation field. From Eq. (29) the real and imaginary parts of the inverse dielectric function in $(\mathbf{K},\Omega)$ space are given, respectively, by

$$\mathrm{Re}\left[\frac{1}{\epsilon(\mathbf{Q},\Omega)}\right] = \sum_{m=-\infty}^{\infty} \frac{J_m^2(r_0 q_x)[1 - V(Q)\mathrm{Re}\,\Pi_0(Q,\Omega+m\omega)]}{[1 - V(Q)\mathrm{Re}\,\Pi_0(Q,\Omega+m\omega)]^2 + [V(Q)\mathrm{Im}\,\Pi_0(Q,\Omega+m\omega)]^2}, \tag{30a}$$

and

$$\mathrm{Im}\left[\frac{1}{\epsilon(\mathbf{Q},\Omega)}\right] = \sum_{m=-\infty}^{\infty} \frac{J_m^2(r_0 q_x)[V(Q)\mathrm{Im}\,\Pi_0(Q,\Omega+m\omega)]}{[1 - V(Q)\mathrm{Re}\,\Pi_0(Q,\Omega+m\omega)]^2 + [V(Q)\mathrm{Im}\,\Pi_0(Q,\Omega+m\omega)]^2}. \tag{30b}$$

Furthermore, the dielectric function in $(\mathbf{K},\Omega)$ space is given by

$$\epsilon(\mathbf{Q},\Omega) = \frac{\displaystyle\prod_{m=-\infty}^{\infty} [1 - V(Q)\Pi_0(Q,\Omega+m\omega)]}{\displaystyle\sum_{m=-\infty}^{\infty} J_m^2(r_0 q_x) \prod_{j=-\infty,\ j\neq m}^{\infty} [1 - V(Q)\Pi_0(Q,\Omega+j\omega)]}. \tag{31}$$

The RPA dielectric function in the $(\mathbf{K},\Omega)$ representation, obtained here from using the diagrams in $(\mathbf{K},t)$ space (given by Fig. 6) and then doing the Fourier transform of it, differs from that obtained from using directly the RPA diagrams in $(\mathbf{K},\Omega)$ space with the pair bubble in the $(\mathbf{K},\Omega)$ representation. For the case where the radiation field is absent, there is no difference of the final result determined by these two approaches. When a time-dependent external field is applied to an electron gas, the response of an electron to the driving field applied depends not only on the time difference $t-t'$ but also on the time shift induced by the time-dependent field. As a result, the Fourier transform done at different stages may lead to different final results. The theoretical approaches used in the present study to determine the quantities such as the Green's function, the d-d correlation function, and the inverse dielectric function in the $(\mathbf{K},\Omega)$ presentation from those obtained in $(\mathbf{K},t)$ space are essentially equivalent to the fast approximation[17] employed for the Fourier analysis

according to time ''center of mass'' [i.e., $\mathcal{T}=(t+t')/2$] and relative coordinates (i.e., $\tau=t-t'$). For the case of an e.m. radiation field that is periodic in time, the usage of generating $e^{ix\cos y}$ and $e^{ix\sin y}$ in the Bessel functions results in the complete spectrum of an electronic quantity being present in the τ direction and only the zeroth term of it existing in the $\mathcal{T}$ direction (here $\mathcal{T}=t'$).

B. Analytical results

For small values of Q (i.e., $Q\ll1$) and in the low-temperature limit ($T\rightarrow0$), we have $\mathrm{Im}\,\Pi_0(\mathbf{Q},\Omega)=0$ and

$$P_m(Q) = V(Q)\mathrm{Re}\,\Pi_0(Q,\Omega+m\omega)$$
$$\simeq \frac{\Omega_p^2}{(\Omega+m\omega)^2} \left[1 + \frac{\mathcal{A}}{(\Omega+m\omega)^2} + O(Q^4)\right], \tag{32}$$

where

$$\Omega_p = \omega_p \Theta(E_F - 2\gamma\hbar\omega) \frac{K_F^{*3/2}}{(3\pi^2 n_e)^{1/2}} \qquad (33)$$

and $\omega_p = (4\pi e^2 n_e / \kappa m^*)^{1/2}$ is the plasmon frequency in the absence of the radiation field. For small values of q_x so that $r_0 q_x \ll 1$, we have

$$J_m^2(r_0 q_x) \simeq \delta_{m,0} + \frac{(r_0 q_x)^2}{4}(\delta_{m,1} - 2\delta_{m,0} + \delta_{m,-1}) + O(q_x^4). \qquad (34)$$

Here the contributions up to the $\mathbf{Q}^2$ term have been included through $\mathcal{A} \sim Q^2$ in Eq. (32) and q_x^2 in Eq. (34). Thus the real part of the dielectric function becomes

$$\mathrm{Re}\ \epsilon(\mathbf{Q},\Omega) \simeq \frac{[1 - P_1(Q)][1 - P_0(Q)][1 - P_{-1}(Q)]}{[1 - P_1(Q)][1 - P_{-1}(Q)] + c\mathcal{B}}, \qquad (35)$$

where $\mathcal{B} \sim q_x^2$ and $c = \Omega_p^2(3\Omega^2 + \Omega_p^2 - \omega^2)/[\Omega^2(\Omega^2 - \omega^2)^2]$.

The collective excitation spectrum induced by the charge-density excitation is determined by the condition of the vanishing of the real part of the dielectric function, namely, by $\mathrm{Re}\ \epsilon(\mathbf{Q},\Omega) \to 0$. For the case of $Q = 0$ (and thus $\mathcal{A} = \mathcal{B} = 0$), we have $\Omega = \Omega_p$, which indicates that in the presence of the e.m. radiations, Ω_p given by Eq. (33) is the plasmon frequency in the long-wavelength limit. Under the e.m. radiations, the plasmon frequency is the functional form of the radiation frequency and intensity. When $F_0 = 0$, $\Omega_p = \omega_p$. Furthermore, in the $Q \to 0$ limit, only the zero-photon process contributes to the plasmon excitation, without taking into consideration the dependence of the Fermi energy on different optical processes.

From Eq. (35) we see that when the $\mathbf{Q}^2$ terms are taken into account in the dielectric function, the plasmon frequency is determined by the condition $[1 - P_1(Q)][1 - P_0(Q)][1 - P_{-1}(Q)] = 0$ induced, respectively, by one-photon absorption, zero-photon emission and one-photon emission. In this case, three plasmon frequencies corresponding to different optical processes can be observed, which are given by

$$\Omega_m(Q) = -m\omega + \Omega_p\left[1 + \frac{3Q^2 V_F^{*2}}{10\Omega_p^2}\right], \qquad (36)$$

where $m = 1$, 0, and -1.

It should be noted that (i) when $F_0 = 0$ so that $\mathcal{B} = 0$ and $\Omega_p = \omega_p$, the dispersion relation of the plasmon spectrum determined by Eq. (35) becomes $\Omega_0(Q) = \omega_p[1 + 3Q^2 V_F^2/10\omega_p^2 + O(Q^3)]$, the well-known result obtained in the absence of the e.m. radiation[2]; (ii) the plasmon dispersion given by Eq. (36) is valid for the case of $r_0 q_x \ll 1$, $|\hbar\Omega + m\hbar\omega| \gg |E(\mathbf{K}) - E(\mathbf{K}+\mathbf{Q})|$, and $\Omega_p \gg \omega$; (iii) under these conditions, the process of zero-photon emission and that of one-photon emission and absorption give rise to the plasmon modes when the effect is included up to the order of $\mathbf{Q}^2$; and (iv) when the higher orders of Q (e.g., $\mathbf{Q}^4$ terms) are taken into account, one can observe the plasmon modes caused by multiphoton channels. These theoretical results indicate that by measuring the dispersion relation of the plasmon spectrum in an electron gas under intense e.m. radiations, we can study the effect of different photon processes on collective excitations. Moreover, it is interesting to note that for an
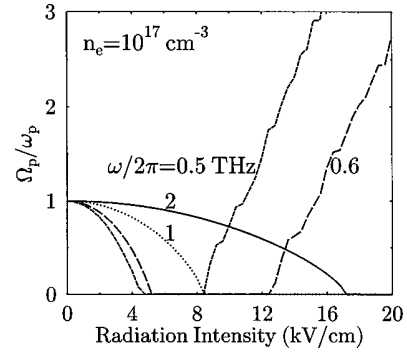

FIG. 7. Plasmon frequency Ω_p as a function of radiation intensity for different radiation frequencies. ω_p is the plasmon frequency in the absence of the e.m. radiation. For GaAs at $n_e = 10^{17}$ cm^{-3}, $\omega_p/2\pi = 3.07$ THz.

electron gas subjected to a linearly polarized e.m. radiation, the electron wave vector (or momentum) along the direction where the radiation field is polarized plays a role in switching channels for different photon processes. The variation of q_x will vary the possibility of the dielectric response occurring around the Fermi level and accompanied by the events of photon emission and absorption. In fact, the electronic transitions, via emission and absorption of photons by electrons, increase with q_x of the electron wave vector. Hence the possibility of the collective excitation associated with a certain optical channel increases with q_x. This also implies that at a fixed radiation field, the intensity of the plasmon excitation via multiphoton transition events increases with increasing electron wave vector (or momentum) along the direction where the radiation field is polarized.

In the present study, I consider only the case of the charge-density excitation by taking into account the real part of the dielectric function alone. The inclusion of the imaginary part of the dielectric function will result in the spin-density excitations that play a role in damping the charge-density excitation and that occur in the relatively large Q case. It is well known that the spin-density excitation, which gives an imaginary part of the excitation spectrum, is relatively weak for semiconductor systems. The physical reason behind this is that the Coulomb interactions cannot flip the electron spin and so the spin-density excitation is very weakly screened. As a result, there are some more strict selection rules for spin-density excitations in comparison to the charge-density excitations. Theoretical results have shown that when the frequency $\Omega + m\omega$ is too large to excite an electron out of the effective Fermi level with only the change of $\mathbf{Q}$, the plasmon modes induced by spin-density excitations are not dissipated rapidly above this frequency.

C. Numerical results

The influence of the FEL radiations on plasmon frequency Ω_p [see Eq. (33)] is shown in Figs. 7 and 8. Plasmons in an electron gas are associated with the single-electron excitations arisen from electronic transitions around the Fermi level, namely, with the processes to excite an electron from an occupied state $|\mathbf{K}\rangle$ to unoccupied states $|\mathbf{K}+\mathbf{Q}\rangle$ with only the change $\mathbf{Q}$ of the electron wave vector. In the presence of the e.m. radiations, these processes can be achieved via op-
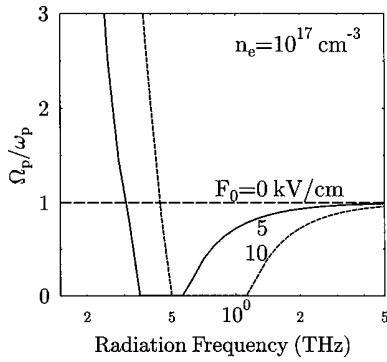
FIG. 8. Plasmon frequency Ω_p as a function of radiation frequency $\omega/2\pi$ for different radiation intensities. ω_p is the plasmon frequency in the absence of the e.m. radiation.

tical absorption and emission by electrons. Under the intense e.m. radiations, due to electron-photon interactions and to dynamical Franz-Keldysh effect, the initial electronic states associated with optical absorption may become unoccupied in some radiation intensity and frequency regimes (see Figs. 4 and 5). In this situation, (i) the Fermi level is below the energy of the radiation field (see Figs. 4 and 5); (ii) the electron DOS and the Fermi energy are mainly determined by the processes of photon emission; (iii) as a result of (i) and (ii), the electronic transitions are mainly accompanied by the events for scattering an electron from an occupied state to unoccupied states via the channels of photon emission; and, consequently, (iv) the electronic excitation is dominated by the emission of photons and the plasmon excitation is suppressed. From Eq. (33) and from Figs. 7 and 8 we see that there is a cutoff of the plasmon frequency in the regime where $E_F - 2\gamma\hbar\omega < 0$. In low-intensity ($F_0 \to 0$ in Fig. 7) and/or high-frequency ($\omega/2\pi > 5$ THz in Fig. 8) radiations, the plasmon frequency depends weakly on the radiation field and $\Omega_p \simeq \omega_p$. With increasing radiation intensity and/or decreasing radiation frequency, the plasmon frequency decreases and reaches the cutoff point due to the reduction of the electronic states for optical absorption. Within the intermediate radiation intensity and frequency regime, the electronic excitation via plasmon modes (photon emission) is less (greatly) possible. From the fact that the dielectric function is connected to the refractive index N of an electron gas, through $N^2 \sim \epsilon(\mathbf{Q},\Omega)$, $\Omega_p \to 0$ (and thus $N \sim 1$) implies that the electron gas is transparent for the radiation. Therefore, I predict here that when the effects of electronic scattering mechanisms (such as impurities and phonons) are not taken into consideration in a 3DEG, there exists a *window* for propagating the terahertz e.m. wave in the intermediate radiation intensities and frequencies. Further increasing F_0 and/or decreasing ω, more and more electronic states for photon absorption become available and the Fermi energy is mainly determined by the energy of the radiation field (see Figs. 4 and 5) because of the larger γ. In this case, the plasmon becomes the major channel for electronic excitations and, consequently, the plasmon frequency increases with increasing radiation intensity and/or with decreasing radiation frequency. An important conclusion that I draw from these results is that using FEL radiations, the frequency tunable

plasmon excitations in semiconductor systems can be achieved by varying the intensity and frequency of the radiation field.

VI. CONCLUSIONS

In this paper, I have derived the Green's function, the density of states, the density-density correlation function, and the dynamical dielectric function for an ideal 3DEG in the $(\mathbf{K},t)$ and $(\mathbf{K},\Omega)$ representations, subject to linearly polarized e.m. radiations. These results are obtained directly from the exact solution of the time-dependent Schrödinger equation. With these results, I have studied the elementary electronic excitation associated with the plasmon oscillation modes via charge-density excitations, by using the usual RPA approach in the $(\mathbf{K},t)$ representation. The dependence of the electron DOS, the Fermi energy, and the plasmon energy on the frequency and intensity of the e.m. radiation has been examined theoretically. The main results obtained from this study are summarized as follows.

Using theoretical approaches developed in this paper, the effect of electron interactions with the radiation field can be included exactly in studying dynamical and steady-state properties of the Green's function, DOS, Fermi energy, dielectric response, collective excitations, etc.

When a GaAs-based 3DEG is subjected to linearly polarized terahertz laser radiations, the electron DOS in the system will be modified strongly by the frequency and intensity of the radiation field. It has been found that the presence of the intense terahertz radiation results in the following. (i) Both optical emission and absorption contribute to the electron DOS. (ii) In the low-energy regime, the DOS comes mainly from the processes of zero-photon and photon emission. The optical processes via channels for absorption of photons affect weakly the DOS (see Fig. 1). (iii) The DOS can be present in the energy regime $E < 0$ due to optical emission, in sharp contrast to the case when the radiation field is absent. (iv) A photon-reduced electron DOS can be observed in the high-energy regime under low-frequency and/or high-intensity radiations (see Figs. 2 and 3).

Due to the strong dependence of the electron DOS on the radiation field, the Fermi energy in a 3DEG will be varied significantly by the frequency and intensity of the e.m. radiation. For a 3DEG subjected to an e.m. radiation field, the energy spectrum of the electronic system becomes $\hbar^2 K^2/2m^* + 2\gamma\hbar\omega$, shifted by the energy $2\gamma\hbar\omega \sim (F_0/\omega)^2$ of the radiation field due to the dynamical Franz-Keldysh effect. I found that (see Figs. 4 and 5) (i) in high-frequency and low-intensity radiation fields where the effect of multiphoton emission and absorption is relatively weak, the Fermi energy E_F is larger than $2\gamma\hbar\omega$; (ii) for a radiation with intermediate frequency and intensity where the electron DOS comes mainly from the processes of photon emission (including multiphoton emissions), E_F may be smaller than $2\gamma\hbar\omega$, the energy of the radiation field, so that the Fermi energy is mainly determined by the channels of optical emission; and (iii) in low-frequency and high-intensity radiations where $2\gamma\hbar\omega \gg \hbar\omega$, the processes of multiphoton emission and absorption affect weakly the Fermi energy and E_F depends strongly on the energy of the radiation field.

A photon-modified Fermi energy will result in a strong

dependence of the plasmon spectrum via, e.g., charge-density excitations, on the frequency and intensity of the radiation field. I found the following (see Figs. 7 and 8). (i) In high-frequency and low-intensity radiations where $E_F > 2\gamma\hbar\omega$, the plasmon frequency Ω_p decreases with increasing radiation intensity and/or with decreasing radiation frequency. (ii) In the intermediate radiation frequency and intensity regime where $E_F < 2\gamma\hbar\omega$, the electronic excitation is achieved mainly via the mechanism of the photon emission and the plasmon excitation is suppressed (i.e., $\Omega_p \sim 0$). In this case, the electron gas becomes transparent for the radiation. This regime is a window for propagation of the e.m. wave with the corresponding intensity and frequency, when the effect of the electronic scattering mechanisms, such as impurities and phonons, are not taken into account. (iii) In low-frequency and high-intensity radiations where $\gamma \gg 1$ and $E_F > 2\gamma\hbar\omega$, Ω_p increases with increasing radiation intensity and/or with decreasing radiation frequency. These results indicate that by varying the intensity and/or frequency of the e.m. radiation, tunable elementary electronic excitations can be achieved in a 3DEG device.

In the presence of the intense terahertz e.m. field polarized linearly, the measurements of the dispersion of plasmon can be used to study the influence of different optical processes on elementary electronic excitations in an electron gas device. With increasing electron wave vector (or momentum) along the direction where the radiation field is polarized, the collective excitation associated with more photon processes becomes possible and so the plasmon modes induced by electronic transitions via multiphoton channels can be observed.

The dramatic terahertz radiation phenomena observed and predicted in this paper can be understood physically by the fact that when a GaAs-based 3DEG is subjected to an intense terahertz e.m. field, the electron kinetic energy, the Fermi energy, the plasmon energy, etc., are comparable to the energy $\hbar\omega$ of photons and to that $2\gamma\hbar\omega$ of the radiation field. As a consequence, (i) the terahertz e.m. field can couple strongly to the electron gas, (ii) the optical processes accompanied by electronic transitions around the Fermi level via emission and absorption of photons become greatly possible, and (iii) the blueshift of the energy spectrum of the electronic system by the radiation via dynamical Franz-Keldysh effect becomes significant. It has been found that the influence of an e.m. radiation on electronic and optical properties of an electron gas device is achieved mainly through two important parameters: $r_0 = eF_0/m^*\omega^2$ and $\gamma = (eF_0)^2/8m^*\hbar\omega^3$. For a GaAs-based 3DEG driven by a linearly polarized e.m. field with $F_0 \sim 1$ kV/cm and $\omega \sim 1$ THz, the conditions such as $r_0 q_x \sim 1$ and $\gamma \sim 1$ can be satisfied. Hence the features distinctive for electron-photon interactions can be exposed.

Finally, the phenomena discussed in this paper are experimentally measurable within the radiation intensity and frequency regimes of free-electron lasers such as the UCSB FEL's (Refs. 6–8) and FELIX.[9–11] We hope that these important terahertz radiation phenomena could be verified experimentally through using the FEL radiations.

*Electronic address: wxu@wumpus.its.uow.edu.au

[1] For a review see, e.g., A. Pinczuk and G. Abstreiter, in *Light Scattering in Solids V*, edited by M. Cardona and G. Guntherodt (Springer-Verlag, Berlin, 1989).

[2] See, e.g., J. M. Ziman, *Principles of the Theory of Solis* (Cambridge University Press, London, 1965).

[3] For a review for the case of 2DEG's see, e.g., T. Ando, A. B. Fowler, and F. Stern, Rev. Mod. Phys. **54**, 437 (1982); I. K. Marmorkos and S. Das Sarma, Phys. Rev. B **48**, 1544 (1993), and references therein.

[4] For the case of 1DEG's see, e.g., Q. P. Li and S. Das Sarma, Phys. Rev. B **43**, 11 768 (1991), and references therein.

[5] For the case of 0DEG's see, e.g., S. A. Mikhailov and V. A. Volkov, Phys. Rev. B **52**, 17 260 (1995), and references therein.

[6] N. G. Asmar, A. G. Markelz, E. G. Gwinn, J. Černe, M. S. Sherwin, K. L. Campman, P. E. Hopkins, and A. C. Gossard, Phys. Rev. B **51**, 18 041 (1995); W. Xu and C. Zhang, Appl. Phys. Lett. **68**, 3305 (1996).

[7] N. G. Asmar, J. Černe, A. G. Markelz, E. G. Gwinn, M. S. Sherwin, K. L. Campman, and A. C. Gossard, Appl. Phys. Lett. **68**, 829 (1996); W. Xu and C. Zhang, Phys. Rev. B **55**, 5259 (1997).

[8] A. G. Markelz, N. G. Asmar, B. Brar, and E. G. Gwinn, Appl.

Phys. Lett. **69**, 3975 (1996); W. Xu, Europhys. Lett. **40**, 411 (1997).

[9] B. N. Murdin, W. Heiss, C. J. G. M. Langerak, S.-C. Lee, I. Galbraith, G. Strasser, E. Gornik, M. Helm, and C. R. Pidgeon, Phys. Rev. B **55**, 5171 (1997).

[10] C. J. G. M. Langerak, B. N. Murdin, B. E. Cole, J. M. Chamberlain, M. Henini, M. Pate, and G. Hill, Appl. Phys. Lett. **67**, 3453 (1995).

[11] T. A. Vaughan, R. J. Nicholas, C. J. G. M. Langerak, B. N. Murdin, C. R. Pidgeon, N. J. Mason, and P. J. Walker, Phys. Rev. B **53**, 16 481 (1996).

[12] A. P. Jauho and K. Johnsen, Phys. Rev. Lett. **76**, 4576 (1996); R. Bertoncini and A. P. Jauho, Phys. Rev. B **44**, 3655 (1991).

[13] See, e.g., R. Shankar, *Principles of Quantum Mechanics* (Plenum, New York, 1980).

[14] See, e.g., J. H. Shirley, Phys. Rev. **138**, 979 (1965).

[15] See, e.g., R. D. Mattuck, *A Guide to Feynman Diagrams in the Many-Body Problem* (McGraw-Hill, New York, 1976).

[16] A. L. Fetter, *Quantum Theory of Many-Particle Systems* (McGraw-Hill, New York, 1971).

[17] See, e.g., T. Brandes, Phys. Rev. B **56**, 1213 (1997), and references therein.